

Preparation and photocatalytic activity of neodymium doping titania loaded to silicon dioxide

YANG Xue-ling, ZHU Li, YANG Le-min, ZHOU Wu-yi, XU Yue-hua

Institute of Biomaterial, College of Science, South China Agricultural University, Guangzhou 510642, China

Received 22 March 2010; accepted 15 August 2010

Abstract: Neodymium doping titania was loaded to silicon dioxide to prepare Nd/TiO₂-SiO₂ by sol-gel method and Nd/TiO₂-SiO₂ was characterized by X-ray diffractometry (XRD), scanning electron microscopy (SEM), Fourier transform-infrared spectroscopy (FT-IR) and diffuse reflectance spectra (DRS). Photocatalytic activities of Nd/TiO₂-SiO₂ with different neodymium contents were evaluated by degradation of methyl orange. The light absorption of Nd/TiO₂-SiO₂ increased with increasing doping neodymium in a visible light range of 388–619 nm, and Nd doping was in favor of decreasing the recombination of photo-generated electrons with holes. Nd and SiO₂ improved the photocatalytic activity of TiO₂. The optimal molar fraction of Nd to Ti was 0.1%, and the optimum calcination temperature was 600 °C. The highest degradation rate of methyl orange was 82.9% after irradiation for 1 h.

Key words: titania; silicon dioxide; neodymium doping; photocatalysis; sol-gel method

1 Introduction

Photocatalysis allows pollution abatement under mild condition (room temperature and pressure), and TiO₂ is the most widely used photocatalyst because of its high photocatalytic activity, non-toxicity, low cost and photochemical stability[1]. However, the light energy used for titania must be equal to or exceed the bandgap of 3.2 eV for anatase, thus, ultraviolet light with wavelength (λ) shorter than 387 nm is required as excitation source[2]. Rare earth ions are known for their f-orbitals to form complexes with various Lewis bases and their oxides having characteristics of adsorption selectivity and thermal stability[3]. In recent years, many groups have examined the effect of rare earth ions doping on photocatalytic properties of TiO₂ and found the bandgap of the catalysts shift into the visible region[4–6]. However, practical applications of photocatalysis are limited because of the difficulty in separation and recycling of TiO₂ powder from the reaction medium. An alternative method is to immobilize TiO₂ powder on supporters, such as glass[7], SiO₂[8] and activated carbon[9]. Supported photocatalysts are often prepared by different methods, such as sol-gel processes[10], liquid phase deposition[11] and

electrochemical deposition[12]. Compared with other methods, sol-gel method presents certain advantages, such as the possibility of deposition onto complex-shaped substrates, obtaining uniform pore size, high pure and homogeneous products at low temperature and easy control of the doping level.

In this work, neodymium doping TiO₂ was loaded to SiO₂ to prepare Nd/TiO₂-SiO₂ using inexpensive SiO₂ as supporter. The Nd/TiO₂-SiO₂ samples were characterized by XRD, SEM, DRS and FT-IR, and their photocatalytic activity to the degradation of methyl orange was also investigated. The aim of this work was to obtain high efficient photocatalysts which were convenient for recycling, and the description of the chemical and physical properties providing a deeper understanding of the photocatalytic mechanism.

2 Experimental

2.1 Preparation of Nd/TiO₂-SiO₂ photocatalysts

Nd/TiO₂-SiO₂ photocatalysts with Nd-doping content from 0.05% to 0.8% (molar fraction) were prepared by sol-gel method. The size of commercial SiO₂ particles was in the range of 75–150 μ m. The preparation was carried out as follows: pure alcohol and diethanolamine (DEA) were added to titanium(IV)-

n-butoxide ($\text{Ti}(\text{OBu})_4$), and then a given amount of alcohol solution of neodymium nitrate was added dropwise under stirring for 30 min. The molar ratio of $\text{Ti}(\text{O-Bu})_4$ to EtOH to DEA was 10:234:10. SiO_2 of 2 g was heated at 180 °C in an oven for 2 h and mixed with 50 mL pure alcohol, 0.5 mL redistilled water and 1.2 g cetyltrimethylammonium bromide (CTAB) under stirring at 25 °C. After the adsorption equilibrium was reached over 12 h, the solution of $\text{Ti}(\text{O-Bu})_4$ was added dropwise under ultrasonic treatment for different time. The solution was refluxed and most solvent was evaporated at 50 °C. Then the samples were dried at 70 °C. The above samples were annealed in air at different temperatures for 3 h and sieved using standard sieves with sizes of 0.075 and 0.150 mm, respectively. A series of $\text{Nd}/\text{TiO}_2\text{-SiO}_2$ photocatalysts with Nd-doping content ranging from 0.05% to 0.8% were obtained. $\text{TiO}_2/\text{SiO}_2$ without neodymium nitrate was prepared for comparison.

2.2 Characterization

X-ray diffraction (XRD) spectra were recorded with a MSAL-XD2 diffractometer ($\lambda=0.154\ 06\ \text{nm}$) using Cu K_α radiation and standard Bragg-Brentano diffraction geometry. The morphology was characterized by scanning electron microscope (SEM, FEI-XL30). FT-IR spectra were recorded using a Nicolet-510P infrared spectrophotometer and referenced to KBr. Diffuse reflectance spectra were performed using a HITACHI U-3010 UV-Vis spectrophotometer in the range of 200–700 nm and referenced to BaSO_4 .

2.3 Photocatalytic activity

Aqueous slurries were prepared by adding 0.4 g photocatalyst to 800 mL methyl orange aqueous solution with concentration of 20 mg/L, and irradiations were performed using a high-pressure mercury lamp of 125 W. The aqueous slurries were stirred and bubbled with oxygen for 30 min prior to the irradiation. At 10 min intervals, aliquots of suspension were extracted. The filtrates were analyzed with a spectrophotometer by measuring their absorbances at 465 nm. The methyl orange photocatalytic degradation was evaluated using a plot of c_0/c versus time (t), where c_0 and c denote the methyl orange concentrations at $t=0$ and $t=t$, respectively.

3 Results and discussion

3.1 X-ray diffraction analysis

Fig.1 shows the XRD patterns of 0.1% $\text{Nd}/\text{TiO}_2\text{-SiO}_2$ calcined at different temperatures. The crystal phase of $\text{Nd}/\text{TiO}_2\text{-SiO}_2$ calcined from 450 to 800 °C was all anatase. With further increase of the calcination temperature to 900 °C, $\text{Nd}/\text{TiO}_2\text{-SiO}_2$ was a mixture of

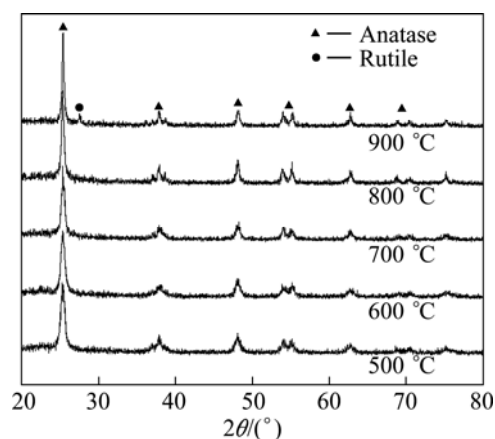


Fig.1 XRD patterns of 0.1% $\text{Nd}/\text{TiO}_2\text{-SiO}_2$ calcined at different temperatures

anatase and rutile. It was shown that $\text{Nd}/\text{TiO}_2\text{-SiO}_2$ displayed good thermal stability because both SiO_2 and Nd inhibited the anatase-rutile phase transformation of TiO_2 [13–14].

3.2 SEM analysis

The SEM images of SiO_2 and 0.1% $\text{Nd}/\text{TiO}_2\text{-SiO}_2$ calcined at 600 °C are shown in Fig.2. Fig.2(a) shows that the surface of commercial SiO_2 was slick, and some nanometer particles were on its surface. Fig.2(b) shows that a layer of Nd/TiO_2 was obvious on the surface of SiO_2 , and its surface was uniform.

3.3 FT-IR spectra analysis

Fig.3 shows the FT-IR spectra of 0.1% $\text{Nd}/\text{TiO}_2\text{-SiO}_2$ calcined at different temperatures. The multiple absorption bands in the region of 420–800 cm^{-1} could be assigned to various vibration modes of Ti-O bond, and the absorption bands at about 3 500 and 1 640 cm^{-1} were attributed to stretching vibrations of physically adsorbed water and hydroxyl. With increasing calcination temperature, the broad peak at 450 cm^{-1} gradually sharpened, indicating the increase of particle size[15], and the absorption band intensity of physically adsorbed water and hydroxyl increased. The broad peaks at 962 and 1 095 cm^{-1} were assigned to the vibration of Si-O-Ti and the asymmetric stretching vibration of Si-O-Si , respectively. The broad peak at 962 cm^{-1} indicated that TiO_2 was supported on the surface of SiO_2 , and a Ti-O-Si bond formed[16].

3.4 DRS analysis

The diffuse reflectance spectra indicated the effect of Nd-doping content on the UV-vis absorption of $\text{Nd}/\text{TiO}_2\text{-SiO}_2$ calcined at 600 °C, as shown in Fig.4. It was seen that the light absorption of $\text{Nd}/\text{TiO}_2\text{-SiO}_2$ in the visible region of 506–619 nm (see the inset in Fig.4) was

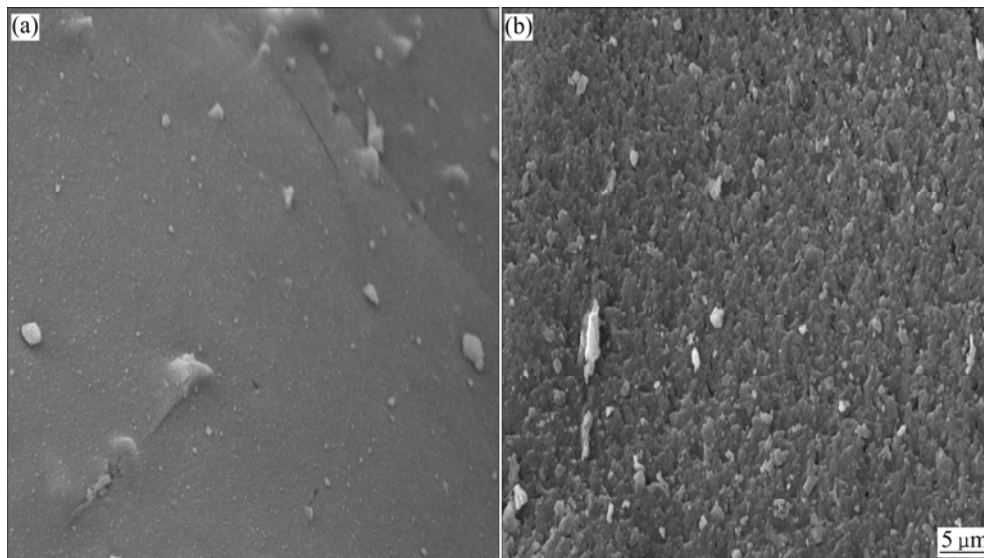


Fig.2 SEM images of SiO₂ (a) and 0.1% Nd/TiO₂-SiO₂ (b)

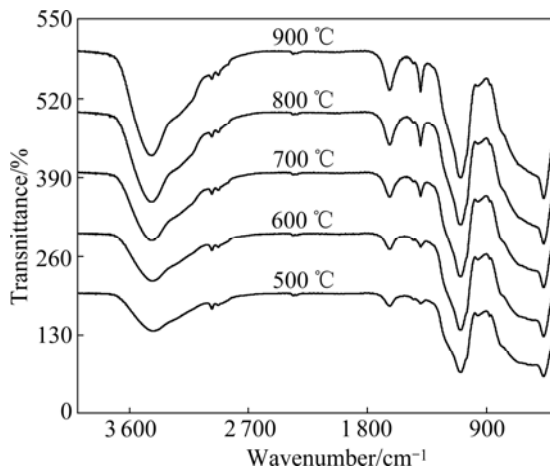


Fig.3 FT-IR spectra of 0.1% Nd/TiO₂-SiO₂ calcined at different temperatures

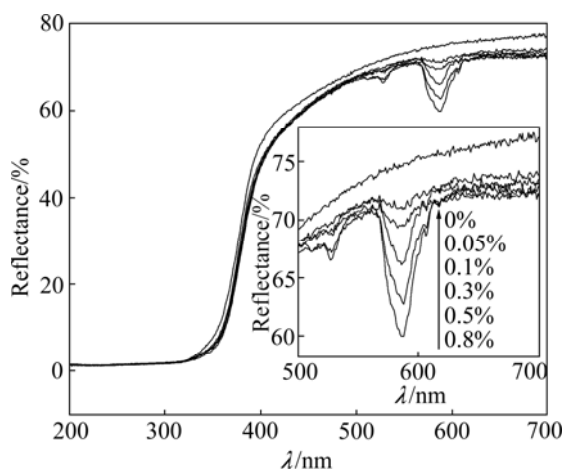


Fig.4 DRS of Nd/TiO₂-SiO₂ with different Nd-doping contents calcined at 600 °C

higher than that of TiO₂-SiO₂, and increased with increasing neodymium content. It was generally thought

that the visible light absorption was caused by the new energy level in the bandgap[17], and the visible light absorption of Nd/TiO₂-SiO₂ could be attributed to the charge transfer between the TiO₂ valence or conduction band and the 4f level of neodymium ion[4, 17]. As a result, Nd/TiO₂-SiO₂ showed a trapping level which decreased the TiO₂ band-gap, and Nd/TiO₂-SiO₂ had visible-light absorption.

3.5 Photocatalytic studies

Fig.5 shows the effect of Nd-doping contents on the photocatalytic activity of Nd/TiO₂-SiO₂. It was shown that the photocatalytic activity of Nd/TiO₂-SiO₂ increased with increasing neodymium content and then decreased when Nd-doping content was up to 0.1%. The optimum Nd-doping content was 0.1%, and the degradation rate of methyl orange was 82.9%. The photocatalytic activity of Nd/TiO₂-SiO₂ was lower than that of TiO₂-SiO₂, and the degradation rate of methyl orange was 72.1% when the Nd-doping amount was up to 0.3%. Metal ions were the acceptors of electrons, and Nd³⁺ could trap photoexcited electrons at the TiO₂ conduction band. So Nd³⁺ could trap electrons to inhibit the recombination of electrons with holes. Moreover, the electrons trapped in Nd³⁺ sites were subsequently transferred to the adsorbed O₂, and the recombination rate of electrons with holes decreased. However, it became the recombination center of electrons with holes, when the neodymium doping content increased further [18]. Consequently, it was understandable that an optimum Nd-doping content existed. The UV-vis spectra showed that the neodymium doping improved the light utilization efficiency of Nd/TiO₂-SiO₂, and generated more electron-hole pairs under light irradiation, which

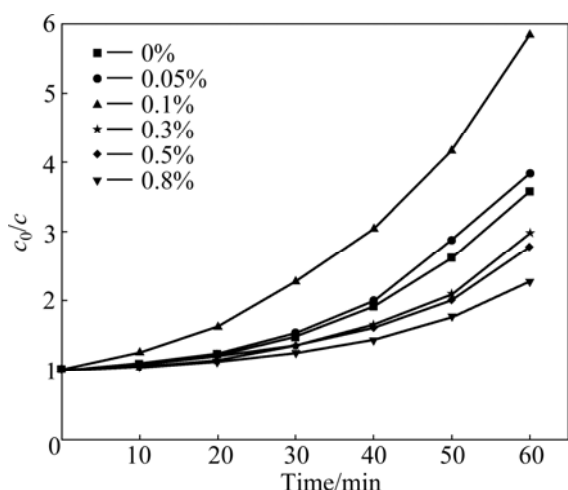


Fig.5 Effect of neodymium content on photocatalytic activity of Nd/TiO₂-SiO₂

helped to enhance the photocatalytic activity of Nd/TiO₂-SiO₂. However, when the Nd-doped content was surplus, even though the visible-light absorption ability was improved, the photocatalytic activity was low due to more recombination centers. At this time, the recombination center of electron-hole pairs was the main factor of photocatalytic activity for photocatalysts.

3.6 Interband photocatalysis mechanism for Nd/TiO₂-SiO₂

Fig.6 shows interband photocatalysis mechanism of Nd/TiO₂-SiO₂ under irradiation by a high-pressure mercury lamp. The atomic f shells of neodymium were partially filled with electrons. The electrons in Nd³⁺ 4f³ orbital which absorbed proper photons energy of visible light could be excited and then transited [19]. A new electronic state in the middle of the TiO₂ band-gap would appear due to neodymium doping. This interband Nd³⁺ trap site in Nd/TiO₂-SiO₂ captured electrons which were excited from the valence band of TiO₂ by absorbing visible-light photons [20]. The 2p electrons of the oxygen anion of oxide generally transited into the valence orbitals of neodymium cations during the charge transfer process (O²⁻ → Nd³⁺). In addition, the irradiation

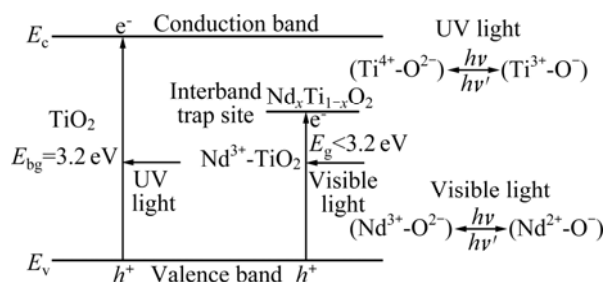


Fig.6 Interband photocatalysis mechanism of Nd/TiO₂-SiO₂ under irradiation by high-pressure mercury lamp

by high-pressure mercury lamp gave rise to the different charge transfer excited state ion-pairs (Nd²⁺-O⁻), which was attributed to the additional interband. Therefore, neodymium doping accelerated the interfacial electron transferring process and changed the band-gap energy of semiconductor TiO₂, and Nd/TiO₂-SiO₂ could be excited by a visible light.

4 Conclusions

1) The crystal phases of Nd/TiO₂-SiO₂ calcined from 450 to 800 °C were all anatase. With further increasing the calcination temperature to 900 °C, Nd/TiO₂-SiO₂ was a mixture of anatase and rutile. Both SiO₂ and Nd inhibited the anatase-rutile phase transformation of TiO₂.

2) FT-IR analysis showed that Ti—O—Si bond in Nd/TiO₂-SiO₂ was formed. Nd/TiO₂-SiO₂ had visible absorption in the range of 400–600 nm, and the light absorption at 584 nm increased with increasing neodymium content. An optimal Nd-doping content was beneficial to decreasing the recombination of photo-generated electrons with holes and enhancing the photocatalytic activity of Nd/TiO₂-SiO₂.

3) 0.1% Nd/TiO₂-SiO₂ calcined at 600 °C exhibited the highest photocatalytic activity to methyl orange photocatalytic oxidation, and the degradation rate of methyl orange was 82.9% after irradiation for 1 h. The high photocatalytic activity of Nd/TiO₂-SiO₂ was mainly attributed to the visible light absorption and the separation of photoexcited electrons and holes.

References

- [1] WANG Feng, MENG Xiang-fu, WEN Bin, ZHANG Jun-hua, DING Yan-fen, ZHANG Shi-min, ZHAO Jin-cai, LIU Shao-ren, YANG Ming-shu. Preparation and photocatalytic activity of PET/TiO₂ hybrid nanofibers via in-situ growth method [J]. Chinese Science Bulletin, 2010, 55(19): 1873–1878. (in Chinese)
- [2] TRAPALIS C C, KEIVANIDIS P, KORDAS G, ZAHARESCU M, CRISAN M, SZATVANYI A, GARTNER M. TiO₂ (Fe³⁺) nanostructured thin films with antibacterial properties [J]. Thin Solid Films, 2003, 433(1–2): 186–190.
- [3] CHEN Jun-tao, LI Xin-jun, YANG Ying, WANG Liang-yan, HE Ming-xing. Effect of Sm³⁺ doping on photocatalytic properties of TiO₂ thin films [J]. Journal of Catalysis 2004, 25(5): 397–402. (in Chinese)
- [4] LIANG Chun-hua, LI Fang-bai, LIU Cheng-shuai, LU Jia-long, WANG Xu-gang. The enhancement of adsorption and photocatalytic activity of rare earth ions doped TiO₂ for the degradation of orange I [J]. Dyes Pigments, 2008, 76(2): 477–484.
- [5] EL-BAHY Z M, ISMAIL A A, MOHAMED R M. Enhancement of titania by doping rare earth for photodegradation of organic dye (Direct Blue) [J]. J Hazard Mater, 2009, 166(1): 138–143.
- [6] KIISK V, SAVEL M, REEDO V, LUKNER A, SILDOS I. Anatase-to-rutile phase transition of samarium-doped TiO₂ powder detected via the luminescence of Sm³⁺ [J]. Phys Procedia, 2009, 2(2): 527–538.

- [7] WANG Ru, XU Yue-hua, CHEN Ming-jie, JIA Jin-liang. Effect of erbium doping on photocatalytic properties of TiO₂ films on glass surface [J]. The Chinese Journal of Nonferrous Metals, 2009, 19(10): 1866–1871. (in Chinese)
- [8] JOSHI U A, CHOI S H, JANG J S, LEE J S. Transesterification of dimethylcarbonate and phenol over silica supported TiO₂ and Ti-MCM 41 catalysts: Structure insensitivity [J]. Catal Lett, 2008, 123: 115–122.
- [9] XU Xin, WANG Xiao-jing, HU Zhong-hua, LIU Ya-fei, WANG Chen-chen, ZHAO Guo-hua. Influence of sol-gel and dip-hydrothermal preparation methods on structure and performance of TiO₂/AC photocatalysts [J]. Acta Physico-Chimica Sinica, 2010, 26(1): 79–86. (in Chinese)
- [10] HOUMARD M, RIASSETTO D, ROUSSEL F, BOURGEOIS A, BERTHOME G, JOUD J C, LANGLET M. Enhanced persistence of natural super-hydrophilicity in TiO₂-SiO₂ composite thin films deposited via a sol-gel route [J]. Surf Sci, 2008, 602: 3364–3374.
- [11] XU Jing-jing, AO Yan-hui, FU De-gang, YUAN Chun-wei. Synthesis of fluorine-doped titania-coated activated carbon under low temperature with high photocatalytic activity under visible light [J]. J Phys Chem Solids, 2008, 69(10): 2366–2370.
- [12] NGUYEN T V, LEE H C, ALAM KHAN M, YANG O B. Electrodeposition of TiO₂/SiO₂ nanocomposite for dye-sensitized solar cell [J]. Sol Energy, 2007, 81(4): 529–534.
- [13] LI Zhi-jie, HOU Bou, XU Yao, WU Dong, SUN Yu-han. Hydrothermal synthesis, characterization, and photocatalytic performance of silica-modified titanium dioxide nanoparticles [J]. J Colloid Interf Sci, 2005, 288(1): 149–154.
- [14] ZHANG Yu-hong, XU Hai-liang, ZHANG Hua-xing, WANG Yan-guang. The effect of lanthanide on the degradation of RB in nanocrystalline Ln/TiO₂ aqueous solution [J]. J Photochem Photobiol A, 2005, 170(3): 279–285.
- [15] SU Wen-yue, FU Xian-zhi, WEI Ke-mei. Photocatalytic degradation of bromomethane on sol-gel derived titania [J]. Chemical Research in Chinese Universities, 2001, 22(2): 272–275. (in Chinese)
- [16] NILCHI A, JANITABAR-DARZI S, MAHJOUB A R, RASOULI-GARMARODI S. New TiO₂/SiO₂ nanocomposites—Phase transformations and photocatalytic studies [J]. Colloid Surface A, 2010, 361(1–3): 25–30.
- [17] XU Y, ZENG Z. The preparation, characterization, and photocatalytic activities of Ce-TiO₂/SiO₂ [J]. J Mol Catal A, 2008, 279(1): 77–81.
- [18] ZHOU Wu-yi, TANG Shao-qiu, ZHANG Shi-ying, ZHOU Xi-rong, WAN Long. Preparation and photocatalytic properties of nano-TiO₂ photocatalysis doped with various rare earth [J]. Journal of the Chinese Ceramic Society, 2004, 32(10): 10–13.
- [19] XIE Yi-bing, YUAN Chun-wei. Photocatalysis of neodymium ion modified TiO₂ sol under visible light irradiation [J]. Appl Surf Sci, 2004, 221: 17–24.
- [20] XIE Yi-bing, YUAN Chun-wei. Visible-light responsive cerium ion modified titania sol and nanocrystallites for X-3B dye photodegradation [J]. Appl Catal B, 2003, 46(2): 251–259.

硅胶负载掺钕 TiO₂ 的制备及其光催化性能

杨学灵, 朱 丽, 杨乐敏, 周武艺, 徐悦华

华南农业大学 理学院 生物材料研究所, 广州 510642

摘 要: 采用溶胶-凝胶法将掺钕二氧化钛负载在二氧化硅上制备复合光催化剂(Nd/TiO₂-SiO₂), 利用 XRD、SEM、FT-IR 和 DRS 对 Nd/TiO₂-SiO₂ 进行表征, 并通过甲基橙溶液的光催化降解评价其光催化性能。结果表明: Nd/TiO₂-SiO₂ 在可见光区 388–619 nm 范围内的光吸收性能随着钕掺杂量的增大而增强, 钕掺杂有利于降低电子-空穴的复合率, 钕和二氧化硅提高 TiO₂ 的光催化活性。在 600 °C 煅烧的 0.1% Nd/TiO₂-SiO₂ 的光催化活性最高, 1 h 后甲基橙降解率为 82.9%。

关键词: 二氧化钛; 二氧化硅; 钕掺杂; 光催化; 溶胶-凝胶法

(Edited by FANG Jing-hua)